

Original scientific paper

PERIODIC SOLUTION OF A MICRO-ELECTROMECHANICAL SYSTEM

Ji-Huan He^{1,2}

¹School of Jia Yang, Zhejiang Shuren University, Hangzhou, Zhejiang, China

²National Engineering Laboratory for Modern Silk,
College of Textile and Clothing Engineering, Soochow University, Suzhou, China

ORCID iD: Ji-Huan He

<https://orcid.org/0000-0002-1636-0559>

Abstract. *This paper examines the periodic motion of the micro-electro-mechanical system (MEMS), which is governed by a singularity that makes it challenging to find an exact solution and to understand its dynamical properties. This paper applies the frequency formulation to gain insight into the frequency-amplitude relationship of the system. It is found that when the amplitude reaches a threshold value, the periodic motion becomes pull-in instability. This finding simplifies the warning system for the system's unsafe operating conditions, and the frequency-amplitude relationship can be used for optimal design of the system with high accuracy and high reliability.*

Key words: MEMS systems, Variational theory, Nonlinear oscillator

1. INTRODUCTION

Micro-electro-mechanical systems (MEMS) have been a driving force in the technological revolution. They are employed in a multitude of cutting-edge applications, including fifth-generation (5G) mobile networks [1], chips [2], ultra-sensitive sensors [3], robots [4], tsunami monitoring [5] and wearable smart fabrics [6,7]. This is due to their extremely simple structure, ultra-finely diminutive size, ultra-light weight, minimal energy consumption, tremendously high reliability, and enormously low cost.

The MEMS system is generally open periodically. However, when the applied voltage exceeds a specified threshold value, the pull-in instability occurs, resulting in system failure. A substantial body of literature exists on the subject of pull-in instability. Mikhasev, et al. studied pull-in instability of carbon nanotube nano-tweezers [8], Tian and her colleagues [9] suggested a new mathematics concept that can control the pull-in instability, and Yang found the pseudo-pull-in stability [10].

Received: June 03, 2024 / Accepted July 07, 2024

Corresponding author: Ji-Huan He

School of Jia Yang, Zhejiang Shuren University, Hangzhou, Zhejiang

E-mail: hejihuan@suda.edu.cn

When the system opens near the pull-in voltage, any minor environmental change may result in a significant shift from normal periodic motion to pull-in motion. This property is widely used for ultrasensitive MEMS-based sensors, which are sensitive to even a small number of nanoparticles in air, or viruses in a room, or even minor environmental changes in, e.g., air velocity, air pressure, poisonous gases, and gravity [3]. It can monitor precisely the propagation of a nano-crack, ground subsidence, the terrestrial plate motion before an earthquake, and other advanced applications, for examples, gas sensors [11], microphones [12], biosensors [13], micro-coils [14], odorant sensors [15], ocean physics [16] and monitoring systems [17]. It is therefore crucial to elucidate its dynamical properties prior to the onset of pull-in motion. This paper will now turn its attention to their periodic motion.

A plethora of analytical techniques exists for the analysis of nonlinear oscillators. These include the variational iteration method [18,19], the homotopy perturbation method [20], the Hamiltonian-based frequency formulation [21], the energy balance method [22], and others. This paper applies the frequency formulation [23] to investigate the periodic properties of the MEMS system.

2. MATHEMATICAL MODEL

Consider a MEMS system as illustrated in Fig. 1, where the micro/nano beam can be a polyvinylidene fluoride (PVDF) nanofiber [24] or metal wire, it locates at the middle of the two symmetrical current-carrying wires. According to the Biot–Savart law [25], the micro/nano beam is under a magnetic force

$$f = \frac{\mu_0 i_1 i_2}{2\pi} \left(\frac{1}{H-w} + \frac{1}{H+w} \right) \quad (1)$$

where f represents the magnetic force per unit length, while μ_0 denotes the magnetic constant. The variables i_1 and i_2 correspond to the direct currents flowing through the wires, while H denotes the distance between them.

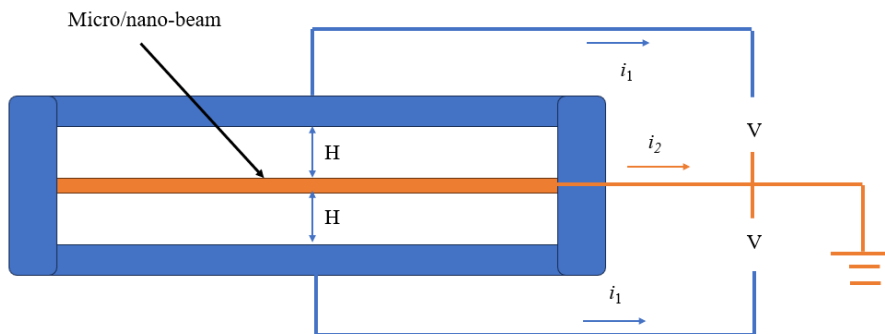


Fig. 1 MEMS system with a simple structure

The governing equation can be expressed as

$$m \frac{d^2 w}{ds^2} + kw = \frac{\mu_0 i_1 i_2 L}{2\pi} \left(\frac{1}{H-w} + \frac{1}{H+w} \right) \quad (2)$$

where m is the mass of the micro/nano beam, k is its elastic coefficient, s is time. Eq. (2) can be written in a dimensionless form:

$$\frac{d^2 u}{dt^2} + u = K \left(\frac{1}{1-u} - \frac{1}{1+u} \right) = \frac{2Ku}{1-u^2} \quad (3)$$

where $u=w/H$, $t=s\omega_0$, $\omega_0=\sqrt{k/m}$, $K= \mu_0 L i_1 i_2 / (2\pi H^2 k)$.

The initial conditions are

$$u(0) = p, \quad u'(0) = q \quad (4)$$

where p and q are constants.

The variational formulation for Eq. (3) is

$$J(u) = \int \left\{ \frac{1}{2} \left(\frac{du}{dt} \right)^2 - \frac{1}{2} u^2 - K [\ln(1-u) + \ln(1+u)] \right\} dt \quad (5)$$

The variational principle for a MEMS system provides an energy approach to insight into the energy conservation during its operation [26]. It is also a useful mathematical tool for complex systems, such as nano-lubrication [27], solitary waves [28], and singular waves [29].

According to the variational formulation of Eq. (5), the following Hamilton function can be obtained:

$$\frac{1}{2} \left(\frac{du}{dt} \right)^2 + \frac{1}{2} u^2 + K [\ln(1-u) + \ln(1+u)] = H \quad (6)$$

where H is Hamilton constant, which depends on the initial conditions of Eq. (4). After identification of H , Eq. (6) becomes

$$\frac{1}{2} \left(\frac{du}{dt} \right)^2 + \frac{1}{2} u^2 + K [\ln(1-u) + \ln(1+u)] = \frac{1}{2} q^2 + \frac{1}{2} p^2 + K [\ln(1-p) + \ln(1+p)] \quad (7)$$

Taking the derivative of this equation with respect to t , we have

$$\frac{du}{dt} \frac{d^2 u}{dt^2} + u \frac{du}{dt} + K \left[\frac{-1}{1-u} + \frac{1}{1+u} \right] \frac{du}{dt} = 0 \quad (8)$$

This equation leads to Eq. (3). Eq. (7) can be used for analysis of the dynamical properties by the Hamiltonian-based frequency formulation [21].

3. FREQUENCY FORMULATION

Considering the following general nonlinear oscillator

$$u'' + h(u, u', u'') = 0 \quad (9)$$

For a periodic solution of Eq. (9), it requires [23]

$$h(0, u', u'') = 0 \quad (10)$$

and

$$h(u, u', u'') / u > 0 \quad (11)$$

We assume that approximate solution is given

$$u(t) = A \cos(\omega t + \phi) \quad (12)$$

where ω is the frequency, A and ϕ can be determined from the initial conditions:

$$A = \sqrt{p^2 + \frac{q^2}{\omega^2}} \quad (13)$$

According to the frequency formulation [23], we have

$$\omega^2 = \frac{h(u, u', u'')}{u} \Bigg|_{\substack{u=NA \\ u'=-A\omega\sqrt{1-N^2} \\ u''=-NA\omega^2}} \quad (14)$$

where A is the amplitude, $0 < N < 1$, in this paper we set $N = \sqrt{3}/2 = 0.8660$. Chun-Hui He and Chao Liu suggested a modification [30]

$$\omega^2 = \frac{\int_0^{T/4} \xi h dt}{\int_0^{T/4} \xi u dt} \quad (15)$$

where ξ is the weighting function. The frequency formulation is the simplest approach to nonlinear vibration systems, it has been successfully applied to various complex oscillators, for examples, fractal vibration systems [31], fractal-fractional oscillators [32], and nonlinear oscillators [33].

For Eq. (3), h can be expressed as

$$h = u - \frac{2Ku}{1-u^2} \quad (16)$$

According to the frequency formulation given in Eq. (14), we have

$$\omega^2 = \left(1 - \frac{2K}{1-u^2}\right)_{u=\sqrt{3}A/2} = 1 - \frac{2K}{1-\frac{3}{4}A^2} = \frac{1-\frac{3}{4}A^2-2K}{1-\frac{3}{4}A^2} \quad (17)$$

For a periodic motion, ω must be positive. When $\omega^2 < 0$, the pull-in motion occurs. So $\omega = 0$ leads to the following critical relationship between the voltage and the amplitude.

$$1 - \frac{3}{4} A^{*2} - 2K^* = 0 \tag{18}$$

where A^* and K^* are, respectively, the critical amplitude and the critical voltage.

$$A^* = \sqrt{\frac{4 - 8K^*}{3}} \tag{19}$$

We can also write Eq. (3) in the form

$$u'' - u''u^2 + u - u^3 - 2Ku = 0 \tag{20}$$

where h can be expressed as

$$h = -u''u^2 + u - u^3 - 2Ku \tag{21}$$

According to the frequency formulation given in Eq. (14), we have

$$\omega^2 = \left[-u''u + 1 - u^2 - 2K \right]_{\substack{u=\sqrt{3}A/2 \\ u'=-\sqrt{3}A\omega/2}} = \frac{3}{4} \omega^2 A^2 + 1 - \frac{3}{4} A^2 - 2K \tag{22}$$

Eq. (22) is equivalent to Eq. (17). In view of Eq. (13), we have the following frequency-amplitude relationship

$$\omega^2 = 1 - \frac{2K}{1 - \frac{3}{4} A^2} = 1 - \frac{2K}{1 - \frac{3}{4} (p^2 + \frac{q^2}{\omega^2})} \tag{23}$$

or

$$\omega = \sqrt{\frac{(4 + 3q^2 - 3p^2 - 8K) + \sqrt{(4 + 3q^2 - 3p^2 - 8K)^2 - 12(4 - 3p^2)q^2}}{2(4 - 3p^2)}} \tag{24}$$

The relationship between the critical voltage K^* and the initial conditions is

$$(4 + 3q^2 - 3p^2 - 8K^*)^2 - 12(4 - 3p^2)q^2 = 0 \tag{25}$$

In order to verify the results, we consider two cases when $p=A=0.1$, $q=0$ and $p=A=0.5$, $q=0$. For the first case, according to Eq. (18), the pull-in voltage can be calculated as

$$K^* = \frac{1}{2} (1 - \frac{3}{4} \times 0.1^2) = 0.49625 \tag{26}$$

While the exact value is $K^*=0.4951$ (see Fig.2a) with a relative error of 0.23%. For the case of $A=0.3$, we have

$$K^* = \frac{1}{2} (1 - \frac{3}{4} \times 0.3^2) = 0.46625 \tag{27}$$

While the exact value is $K^*=0.3751$ (see Fig.2b) with a relative error of 6.75%. For the case of $A=0.5$, we have

$$K^* = \frac{1}{2} (1 - \frac{3}{4} \times 0.5^2) = 0.40625 \tag{28}$$

While the exact value is $K^*=0.5$ (see Fig. 2c) with a relative error of 8.3%.

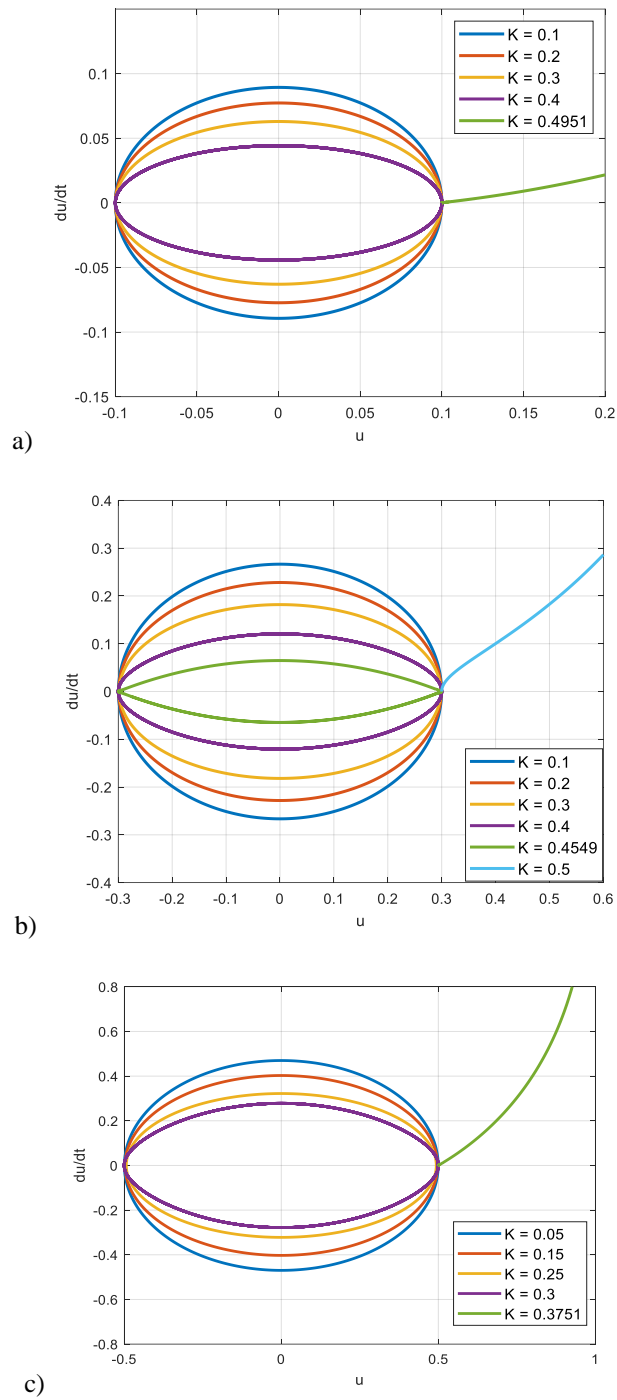


Fig. 2 Phase diagram. (a) $A=0.1$; (b) $A=0.3$ (c) $A=0.5$

To improve the prediction accuracy for K^* , we can use Eq.(7) to give an exact relationship between the critical voltage (K^*) and the critical amplitude (A^*):

$$\frac{1}{2} A^{*2} + K^* [\ln(1 - A^*) + \ln(1 + A^*)] = H \tag{29}$$

where H is determined by the initial conditions

Fig.3, Fig.4 and Fig.5 compare the approximate solutions with the numerical solutions for $A=0.1, 0.3$ and 0.5 , respectively, and a good agreement is found, showing the method is reliable.

It can be found that the errors become larger for a larger K . This is because when $K > K^*$, the pull-in instability occurs, so when K tends to K^* , the periodic motion tends gradually to the pull-in instability.

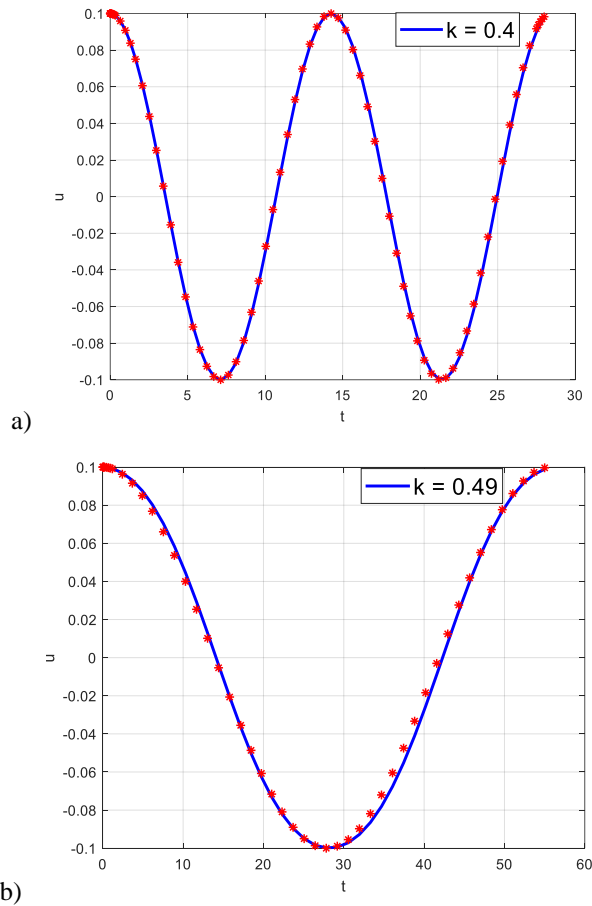


Fig. 3 Exact solution (continued line) vs approximate solution (discontinuous line) for $A=0.1$.
 (a) $K=0.4$; (b) $K=0.49$ with $K^*=0.4951$

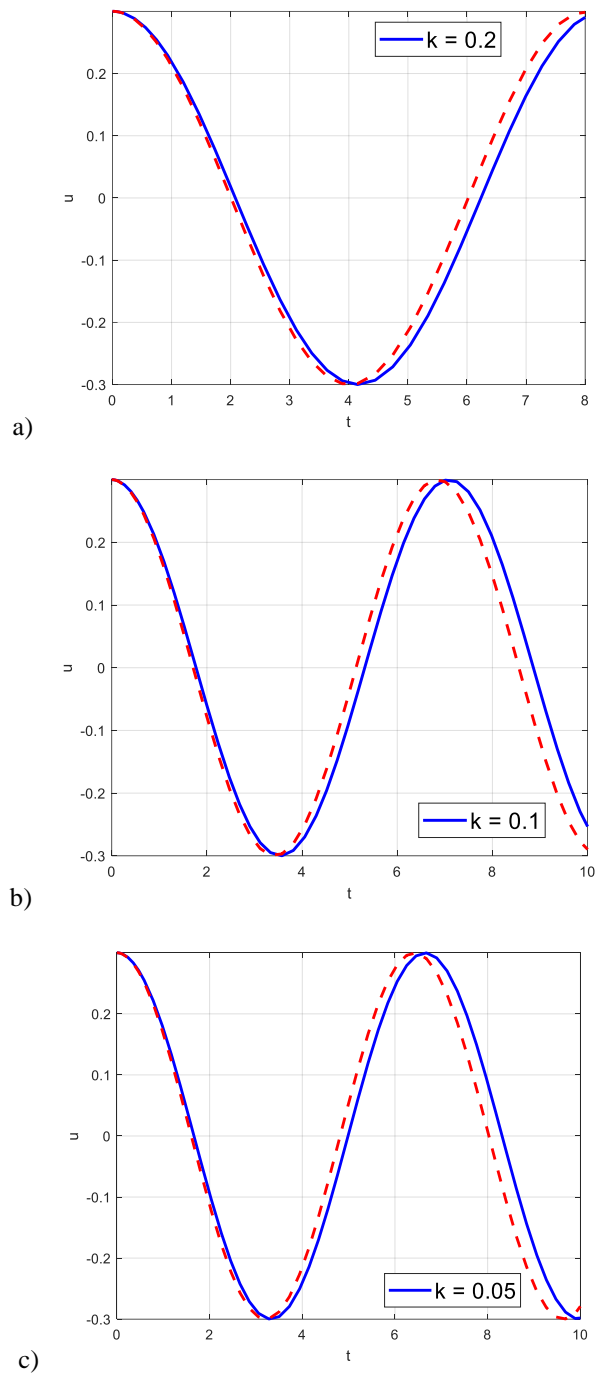
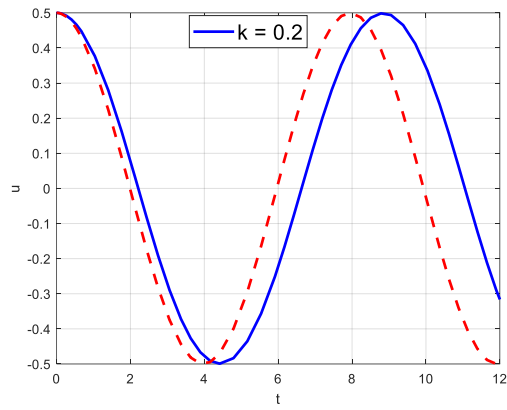
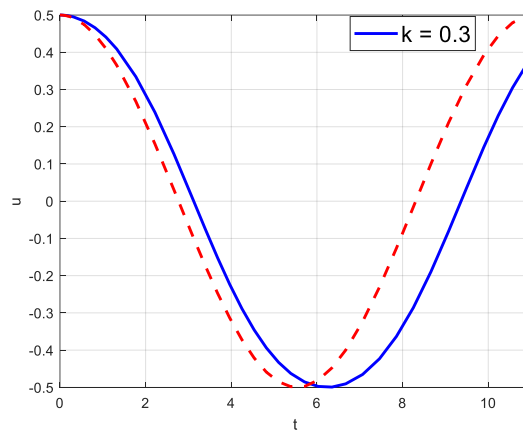


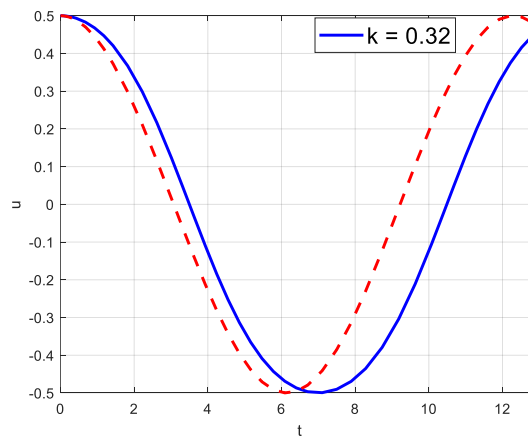
Fig. 4 Exact solution (continued line) vs approximate solution (discontinuous line) for $A=0.3$.
(a) $K=0.2$; (b) $K=0.3$; (c) $K=0.32$ with $K^*=0.50$



a)



b)



c)

Fig. 5 Exact solution (continued line) vs approximate solution (discontinuous line) for $A=0.5$. (a) $K=0.2$; (b) $K=0.3$; (c) $K=0.32$ with $K^*=0.3751$

3. A GENERALIZED MEMS OSCILLATOR

In Fig.1, the wires can be thin plates, in that case, the governing equation can be expressed as [22]

$$EI \frac{\partial^4 w}{\partial x^4} + \rho A \frac{\partial^2 w}{\partial t^2} = \left[N + \frac{ES}{2L} \int_0^L \left(\frac{\partial w}{\partial x} \right)^2 dx \right] \frac{\partial^2 w}{\partial x^2} + \frac{\varepsilon b v^2}{2} \left[\frac{1}{(H-w)^2} + \frac{1}{(H+w)^2} \right] \quad (29)$$

where w is the displacement, EI the stiffness, ρ density, A area, N applied force, L length, S cross-section area, b width, ε dielectric constant, and v the Poisson ratio. In Eq.(29), the last term is the electrostatic excitation.

For the fixed-fixed micro/nano thin plate, the boundary conditions are

$$w(0) = w(L) = 0 \quad \text{and} \quad \frac{dw}{dx}(0) = \frac{dw}{dx}(L) = 0 \quad (30)$$

Considering the boundary conditions of Eq. (30), we assume that w can be expressed as

$$w(t, x) = u(t)x^2(1-x)^2(1+c_1x+c_2x^2+\dots) \quad (31)$$

where c_i ($i=1,2,3,\dots$) are constants. Submitting Eq. (31) into Eq. (29) and integrating the resultant equation with x from 0 to L , we finally have

$$(a_8 u^8 + a_6 u^6 + a_4 u^4 + a_2 u^2 + a_0) \frac{d^2 u}{dt^2} + a_1 u + a_3 u^3 + a_5 u^5 + a_7 u^7 + a_9 u^9 = 0 \quad (32)$$

where a_i ($i=0-9$) are constants.

We re-write Eq. (32) in the form

$$\frac{d^2 u}{dt^2} + \frac{a_1 u + a_3 u^3 + a_5 u^5 + a_7 u^7 + a_9 u^9}{a_8 u^8 + a_6 u^6 + a_4 u^4 + a_2 u^2 + a_0} = 0 \quad (33)$$

The frequency formulation can be modified as

$$\omega^2 = \frac{\int_{\phi}^{\phi+T/4} (a_1 u + a_3 u^3 + a_5 u^5 + a_7 u^7 + a_9 u^9) \cos(\omega t + \phi) dt}{\int_{\phi}^{\phi+T/4} (a_8 u^8 + a_6 u^6 + a_4 u^4 + a_2 u^2 + a_0) u \cos(\omega t + \phi) dt} \quad (34)$$

Submitting Eq. (12) into Eq. (34), after simple calculation, we have

$$\omega^2 = \frac{a_1 + \frac{3}{4} a_3 A^2 + \frac{5}{6} \frac{3}{4} a_5 A^4 + \frac{7}{8} \frac{5}{6} \frac{3}{4} a_7 A^6 + \frac{9}{10} \frac{7}{8} \frac{5}{6} \frac{3}{4} a_9 A^8}{\frac{9}{10} \frac{7}{8} \frac{5}{6} \frac{3}{4} a_8 A^6 + \frac{7}{8} \frac{5}{6} \frac{3}{4} a_6 A^4 + \frac{5}{6} \frac{3}{4} a_4 A^2 + \frac{3}{4} a_2 A^2 + a_0} \quad (35)$$

Additionally, we can write Eq. (32) in the form

$$u'' + \frac{1}{a_0} \left\{ a_1 u + a_3 u^3 + a_5 u^5 + a_7 u^7 + a_9 u^9 - (a_8 u^8 u'' + a_6 u^6 u'' + a_4 u^4 u'' + a_2 u^2 u'') \right\} = 0 \quad (36)$$

By Eq. (14) we have

$$\omega^2 = \frac{a_1 + a_3 u^2 + a_5 u^4 + a_7 u^6 + a_9 u^8 - (a_8 u^7 u'' + a_6 u^5 u'' + a_4 u^3 u'' + a_2 u u'')}{a_0} \Bigg|_{\substack{u=\sqrt{3}A/2 \\ u=-\sqrt{3}A\omega^2/2}} \quad (37)$$

$$= \frac{a_1 + \frac{3}{4} a_3 A^2 + \frac{9}{16} a_5 A^4 + \frac{27}{64} a_7 A^6 + \frac{81}{256} a_9 A^8 - (\frac{81}{256} a_8 A^8 + \frac{27}{64} a_6 A^6 + \frac{9}{16} a_4 A^4 + \frac{3}{4} a_2 A^2) \omega^2}{a_0}$$

After simple operation, Eq. (37) leads to the following frequency-amplitude relationship

$$\omega^2 = \frac{a_1 + \frac{3}{4} a_3 A^2 + \frac{9}{16} a_5 A^4 + \frac{27}{64} a_7 A^6 + \frac{81}{256} a_9 A^8}{a_0 + \frac{81}{256} a_8 A^8 + \frac{27}{64} a_6 A^6 + \frac{9}{16} a_4 A^4 + \frac{3}{4} a_2 A^2} \quad (38)$$

Eq. (35) or Eq. (38) unlocks the frequency-amplitude relationship, and in view of Eq.(13), we can also reveal the effect of the initial conditions on the frequency property.

4. CONCLUSION

This paper studies the frequency property of MEMS systems, its frequency-amplitude relationship is revealed, and the effect of the initial conditions on the frequency property is also elucidated. When the obtained frequency is zero, we can easily obtain the threshold value for K in Eq. (3), beyond which the pull-in instability occurs. The threshold value for the amplitude is also found, this makes it easy to monitor MEMS systems, and it can set off an alarm when the amplitude approaches to its threshold value.

REFERENCES

1. Iannacci, J., 2023, *Modelling, validation and experimental analysis of diverse RF-MEMS ohmic switch designs in view of beyond-5G, 6G and future networks—Part 1*, Sensors, 23, 3380.
2. Zhang, X.S., Kwon, K., Henriksson, J., Luo, J.H., Wu, M.C., 2022, *A large-scale microelectromechanical-systems-based silicon photonics LiDAR*, Nature, 603, 253-258.
3. He, J.H., He, C.H., Qian, M.Y., Alsolami, A.A., 2024, *Piezoelectric Biosensor based on ultrasensitive MEMS system*, Sensors and Actuators A: Physical, 376, 115664.
4. Valles, A.E., Alva, V.R., Belokonov, I., 2023, *Calibration method of MEMS gyroscopes using a robot manipulator*, Aerospace and Electronic System Magazine, 38(3), pp. 20-27.
5. Middlemiss, R.P., Samarelli, A., Paul, D.J., et al., 2016, *Measurement of the Earth tides with a MEMS gravimeter*, Nature, 531, pp. 614-617.
6. Gu, W., Hou, C.Y., Zhang, Q.H., et al., 2019, *Present situation and development trend of intelligent garment*, Journal of Donghua University (Natural Science), 45(6), pp. 837-843.
7. Zheng, C., Zou, Y.L., Hu, J.Y., 2021, et al. *Research advances in wearable NFC fabric antenna and energy transfer*, Journal of Donghua University (Natural Science), 47(5), pp. 37-46.
8. Mikhasev, G., Radi, E., Misnik, V., 2024, *Modeling pull-in instability of CNT nanotweezers under electrostatic and van der Waals attractions based on the nonlocal theory of elasticity*, International Journal of Engineering Science, 195, 104012.
9. Tian, D., Ain, Q.T., Anjum, N., et al., 2021, *Fractal N/MEMS: from pull-in instability to pull-in stability*, Fractals, 29(2), 2150030.
10. Yang, Q., 2023, *A mathematical control for the pseudo-pull-in stability arising in a micro-electromechanical system*, Journal of Low Frequency Noise, Vibration and Active Control, 42(2), pp. 927-934.
11. Ghommam, M., Hemid, M., Alattar, B., et al., *Development of MEMS gas sensors equipped with metal organic frameworks*, Sensors and Actuators A: Physical, 371, 115296.

12. Shubham, S., Nawaz, M., Song, X., et al., 2024, *A behavioral nonlinear modeling implementation for MEMS capacitive microphones*, Sensors and Actuators A: Physical, 371, 115294.
13. Wang, C.L. and Madou, M., 2005, *From MEMS to NEMS with carbon*, Biosensors & Bioelectronics, 20(10), pp. 2181-2187.
14. Liu, X.Y., Whalen, A.J., Kim, K., et al., 2023, *MEMS micro-coils for magnetic neurostimulation*, Biosensors & Bioelectronics, 227, 115143.
15. Manai, R., Scorsone, E., Rousseau, L., et al., 2014, *Grafting odorant binding proteins on diamond bio-MEMS*, Biosensors & Bioelectronics, 60, pp. 311-317.
16. Yang, Y., Dai, Z.H., Chen, Y., et al., 2024, *Emerging MEMS sensors for ocean physics: Principles, materials, and applications*, Applied Physics Reviews, 11(2), 021320.
17. Qin, X., Tang, L.D., 2024, *An Environmental Monitoring Method of Ancient Buildings Based on the Micro Electro Mechanical System Accelerometers*, Journal of Nanoelectronics and Optoelectronics, 19(1), pp. 36-45.
18. Feng, G.Q., Zhang, L., Tang, W., 2023, *Fractal pull-in motion of electrostatic MEMS resonators by the variational iteration method*, Fractals, 31(9), 2350122.
19. Anjum, N., Rasheed, A., He, J.H., Alsolami, A.A., 2024, *Free Vibration of a Tapered Beam by the Aboodh Transform-based Variational Iteration Method*, Journal of Computational Applied Mechanics, 55(3), pp. 440-450.
20. He, C.H., El-Dib, Y.O., 2022, *A heuristic review on the homotopy perturbation method for non-conservative oscillators*, Journal of Low Frequency Noise, Vibration & Active Control, 41(2), pp. 572-603.
21. Ma, H.J., 2022, *Simplified Hamiltonian-based frequency-amplitude formulation for nonlinear vibration systems*, Facta Universitatis-Series Mechanical Engineering, 20(2), pp. 445-455.
22. Fu, Y., Zhang, J., Wan, L., 2011, *Application of the energy balance method to a nonlinear oscillator arising in the microelectromechanical system (MEMS)*, Current Applied Physics, 11(3), pp. 482-485
23. He, J.H., 2019, *The simplest approach to nonlinear oscillators*. Results Phys., 15,102546.
24. Zhong, X.J., Li, W.L., Gao, X., et al., 2024, *Preparation and output performance of triboelectric nanogenerator based on electrospun PVDF/GO composite nanofibers*, Journal of Donghua University (Natural Science), 50(3), pp. 15-22.
25. Skrzypacz, P., Kadyrov, S., Nurakhmetov, D., et al., 2019, *Analysis of dynamic pull-in voltage of a graphene MEMS model*. Nonlinear Anal Real World Appl , 45, pp. 581–589.
26. He, C.H., 2023, *A variational principle for a fractal nano/microelectromechanical (N/MEMS) system*, Int. J. Numer. Method. H., 33(1), pp. 351-359.
27. Zuo, Y.T., 2024, *Variational principle for a fractal lubrication problem*, Fractals, doi: 10.1142/S0218348X24500804.
28. Wang, K.L., He, C.H., 2019, *A remark on Wang's fractal variational principle*, Fractals, 27(8), 1950134.
29. He, C.H., Liu, C., 2023, *Variational principle for singular waves*, Chaos, Solitons & Fractals, 172, 113566.
30. He, C.H., Liu, C., 2022, *A modified frequency-amplitude formulation for fractal vibration systems*, Fractals, 30(3): 2250046.
31. Tian, Y., 2022, *Frequency formula for a class of fractal vibration system*, Reports in Mechanical Engineering, 3(1), pp. 55-61.
32. Niu, J.-Y., Feng, G.-Q., Gepreel, K.A., 2023, *A simple frequency formulation for fractal–fractional non-linear oscillators: A promising tool and its future challenge*. Front. Phys. 11, 1158121.
33. El-Dib, Y.O., 2024, *A review of the frequency-amplitude formula for nonlinear oscillators and its advancements*. Journal of Low Frequency Noise, Vibration and Active Control, doi:10.1177/14613484241244992.